Fast orthorectification method using multi-pixel chunking

Guoqing Zhou[a,b], Haoran Li[a,b], Qingyang Wang[a,b]
[a] Guangxi Key Laboratory of Spatial Information and Geomatics, Guilin University of Technology, Guilin 541004, China; [b] College of Geomatics and Geoinformation, Guilin University of Technology, Guilin 541004, China

ABSTRACT

The traditional digital differential orthorectification uses a pixel-by-pixel correction method, which is time-consuming and laborious to operate on a single image element and fails to meet the demand for time-sensitive and near real-time DOM production generation. In order to solve this problem, a fast DOM generation method based on multi-pixel binning is investigated in this paper. The method breaks the shackles of the traditional digital differential correction, which only operates on individual pixels, and instead corrects blocks of N×N size, greatly improving the speed of DOM generation processing. The dataset used in this paper are aerial imagery and a DSM of LiDAR acquisition located in Denver, Colorado, USA, to verify the speed and accuracy of the algorithm proposed. Compared with the traditional digital differential correction method, the speed of DOM generation using this method is dependent on the pixel chunk size. The orthorectification speed about 4.1 times faster than the traditional method when using a 3×3 pixels chunks, and about 9.8 times faster than the traditional method when using a 7×7 pixels chunks.

Keywords: ortho-rectification, digital differentiation correction, pixel operation

1. INTRODUCTION

Orthorectification is the process of correcting the original image of the central projection to a vertical planimetric map and eliminating the parallax caused by topographic features. As a key component of the national spatial data infrastructure, digital ortho map (DOM) has both the geometric accuracy of a map and the characteristics of image vision [1-3]. A high-precision digital orthophoto has important practical significance for urban construction planning, ecological environment investigation and monitoring.

Many scholars have conducted orthorectification studies in recent decades, and Zhou et al. have conducted a comprehensive study of the theory, algorithms, and methods for large-scale urban orthophoto generation [4]. Aguilar et al. evaluated the accuracy of GeoEye-1 and WorldView-2 images by orthotropic correction using a strict model and a rational function model. The results showed that the optimal correction accuracy could be obtained using a third-order rational function model with RPC coefficients provided by the supplier [5]. Habib et al. proposed a method to improve the quality of UAV orthophotos using frame cameras and hyperspectral imagers [6]. However, these studies of orthorectification methods are based on traditional image processing systems, which cannot satisfy the demand for fast and real-time image processing.

In recent years, in order to meet the application of disaster relief, military deployment and other situations, the demand for fast and real-time remote sensing image orthographic correction is increasing. To improve the image processing speed, researchers have proposed various parallel processing and hardware acceleration methods [7-11]. For example, Warpenburg and Siegel perform resampling in the single-instruction multi-data stream environment [12]. Wittenbrink et al. proposed an optimal read-write parallel access algorithm for spatial image distortion [13]. Liu et al. proposed an orthophoto correction parallel processing algorithm for a large number of remote sensing images [14]. Dai and Yang propose an ortho correction algorithm based on co-processing of central processing unit (CPU) and graphics processing unit (GPU) [15]. Quan et al. proposed a GPU-accelerated parallel algorithm for orthographic correction of optical aerial images. These methods can improve the processing speed of ortho correction to some extent [16]. These methods improve the processing speed of ortho correction to some extent. However, most of these parallel processing methods are GPU-based multitasking operating systems, which cannot essentially solve the problems of serial instruction methods and require high hardware requirements. That is why the above method has not gained popularity in commerce.

SPIE-CLP Conference on Advanced Photonics 2022, edited by Xu Liu, Anatoly Zayats, Xiaocong Yuan, Proc. of SPIE Vol. 12601, 126010I
© 2023 SPIE · 0277-786X · doi: 10.1117/12.2666099

To address the above problems, this paper proposes a fast orthorectification method based on multi-pixel chunking. The method in this paper simultaneously performs indirect method digital correction for N×N size pixel blocks, which can significantly improve the processing speed. The accuracy and speed of the proposed method are validated by taking an aerial image of downtown Denver, Colorado as an example.

2. ORTHOGRAPHIC CORRECTION OF MULTI-PIXEL CHUNKS

The specific process of orthorectification for multi-pixel chunking is as follows.

(1) Calculate the corrected image extent and size from DSM data.

(2) Determine the pixel chunk size (e.g., 7*7 pixels as a pixel chunk) and create a blank orthophoto based on the resolution and chunk size. Then chunk the blank orthophoto.

(3) Calculate the coordinates of the ground points corresponding to each chunk of the corrected image. Starting from the corrected image, assume that the corrected image is arbitrarily chunked B_{ij} (denoting the block of pixels in the i-th row and j-th column). Its lower left corner corresponding geodesic coordinates ($X_{L_{ij}}, Y_{L_{ij}}$) and the central image point corresponding geodesic coordinates ($X_{C_{ij}}, Y_{C_{ij}}$) can be calculated from the starting point of DSM with orthophoto resolution, as in Eq. 1:

$$\begin{cases} X_{L_{ij}} = X_0 + (j-1)NM\,, \quad Y_{L_{ij}} = Y_0 + (i-1)NM \\ X_{C_{ij}} = X_0 + \frac{j(N+1)M}{2}\,, \quad Y_{C_{ij}} = Y_0 + \frac{i(N+1)M}{2} \end{cases} \tag{1}$$

where (X_0, Y_0) is the starting angle point of the lower left corner of the DSM, M is the resolution of the orthophoto, and N is the pixel chunk size (N must be an odd number, e.g., $N = 7$ for 7×7 pixel chunks).

According to equation (1), the actual ground extent corresponding to B_{ij} can be expressed as:

$$B_{ij} \in \left\{ X_{L_{ij}} \leq X \leq X_{L_{(i+1)(j+1)}}\,, Y_{L_{ij}} \leq Y \leq Y_{L_{(i+1)(j+1)}} \right\} \tag{2}$$

(4) Calculate the image point coordinates. Create an N×N matrix for B_{ij}. Considering the high accuracy requirement of orthophoto processing, the elevation values can be obtained by interpolating the existing DSM data. The central image point $(x_{C_{ij}}, y_{C_{ij}})$ is calculated as follows, and $(x_{L_{ij}}, y_{L_{ij}})$ is calculated in the same way without further elaboration:

$$x_{C_{ij}} = -f \frac{a_1\left(X_{C_{ij}} - X_S\right) + b_1\left(Y_{C_{ij}} - Y_S\right) + c_1\left(Z_{C_{ij}} - Z_S\right)}{a_3\left(X_{C_{ij}} - X_S\right) + b_3\left(Y_{C_{ij}} - Y_S\right) + c_3\left(Z_{C_{ij}} - Z_S\right)} + x_0 \tag{3}$$

$$y_{C_{ij}} = -f \frac{a_2\left(X_{C_{ij}} - X_S\right) + b_2\left(Y_{C_{ij}} - Y_S\right) + c_2\left(Z_{C_{ij}} - Z_S\right)}{a_3\left(X_{C_{ij}} - X_S\right) + b_3\left(Y_{C_{ij}} - Y_S\right) + c_3\left(Z_{C_{ij}} - Z_S\right)} + y_0 \tag{4}$$

where f, x_0, y_0 denote the internal orientation element parameters of the camera, X_S, Y_S, Z_S denote the center position of the camera, and $a1, \dots, c3$ denote the rotation matrix.

(5) Get the grayscale value. From equations (3-4), the coordinates of the image point $(x_{C_{ij}}, y_{C_{ij}})$, $(x_{L_{ij}}, y_{L_{ij}})$ of the lower left corner as well as the center of each sub-block B_{ij} can be obtained, and the transformation of the object-side coordinates to the image-side coordinates will be deflected, as shown in Fig 1.

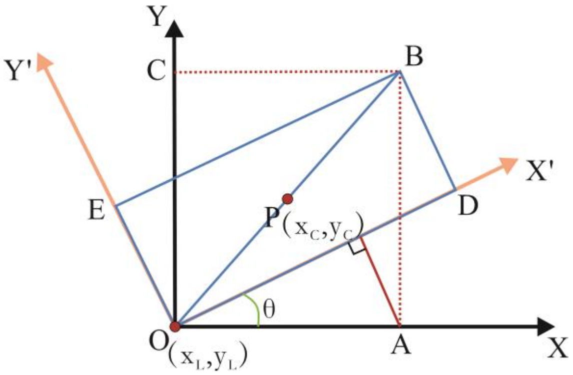

Fig.1 Pixel block deflection schematic

It can be seen in the Fig.1 that $(x_{L_{ij}}, y_{L_{ij}})$ and $(x_{C_{ij}}, y_{C_{ij}})$ obtained by equations (3-4) correspond to the points O and P in the figure. If there is no deflection then it is easy to calculate that B_{ij} corresponds to the rectangle OABC, but in the actual case B_{ij} should correspond to the rectangle ODBE. Since the length of the diagonal OB is fixed, the range of the rectangle ODBE can be obtained by simply calculating the projection of OB on the new coordinate axis. And the pixel blocks are deflected in the same direction in the same image during the correction process so only θ needs to be calculated once. From the geometric relations, the rotation matrix R is calculated as follows:

$$R = \begin{bmatrix} \cos\theta & \sin\theta \\ -\sin\theta & \cos\theta \end{bmatrix} \tag{5}$$

Then the span of B_{ij} neighboring pixels on the original image ranks is calculated as in the following equation:

$$r_{ij} = \frac{2\left|x_{C_{ij}} - x_{L_{ij}}\right|}{N-1} \tag{6}$$

$$c_{ij} = \frac{2\left|y_{C_{ij}} - y_{L_{ij}}\right|}{N-1} \tag{7}$$

where r_{ij} denotes the pixel span of B_{ij} neighboring pixels on the rows corresponding to the original image, and c_{ij} denotes the pixel span of B_{ij} neighboring pixels on the columns corresponding to the original image.

Based on the pixel span and pixel block rotation matrix of B_{ij} on the original image obtained from equations (5-7), the pixel coordinates of each element in B_{ij} corresponding to the original image can be calculated as follows:

$$B_{ij} = R\begin{bmatrix} (x_{L_{ij}}, y_{L_{ij}} + Nr_{ij}) & & \cdots & & (x_{L_{ij}} + Nc_{ij}, y_{L_{ij}} + Nr_{ij}) \\ (x_{L_{ij}}, y_{L_{ij}} + (N-1)r_{ij}) & \cdots & (x_{C_{ij}}, y_{C_{ij}} + r_{ij}) & \cdots & (x_{L_{ij}} + Nc_{ij}, y_{L_{ij}} + (N-1)r_{ij}) \\ \vdots & & (x_{C_{ij}}, y_{C_{ij}}) & & \vdots \\ (x_{L_{ij}}, y_{L_{ij}}) & & \cdots & & (x_{L_{ij}} + Nc_{ij}, y_{L_{ij}}) \end{bmatrix} \tag{8}$$

Since the location of the pixel block B_{ij} corresponding to the image point of the original image may not fall in the center of the image element, a grayscale interpolation is needed for this purpose and generally using bilinear interpolation. Finally, the grayscale value on the obtained original image is assigned to the corrected image. The overall process is shown in Figure 2.

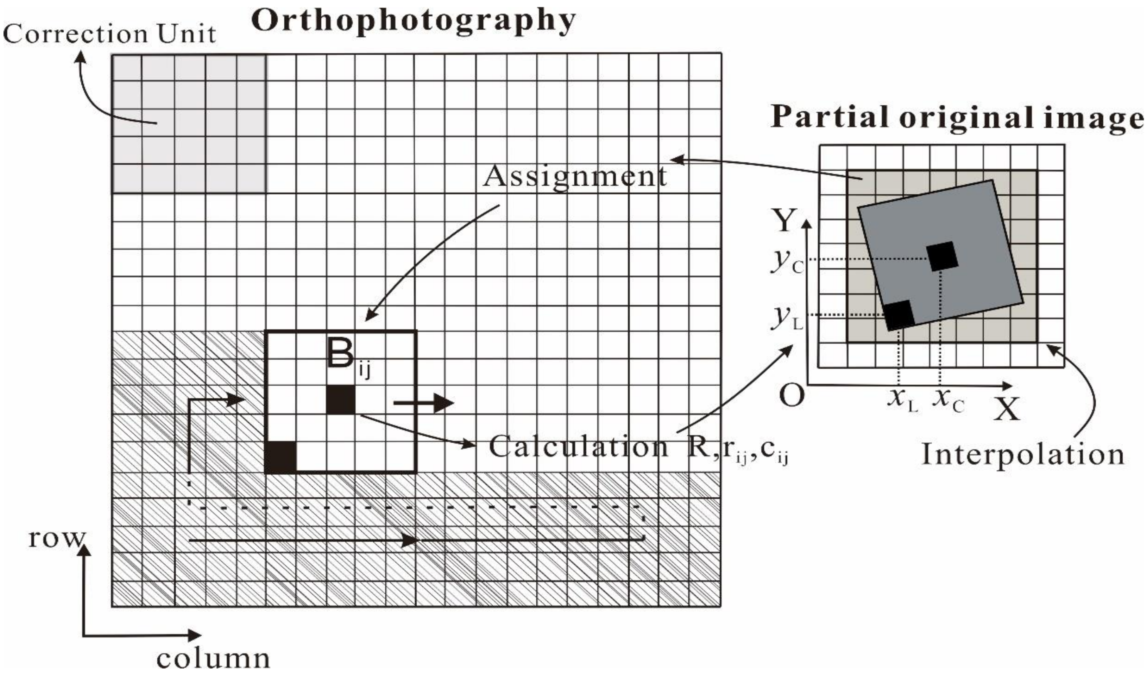

Fig.2 Pixel chunking de correction principle (5*5 pixels chunking size as an example)

3. EXPERIMENTS AND RESULTS

3.1 Experimental data

The experimental area selected for this paper is located in the center of Denver, Colorado, and the data used include digital surface model data (DSM), and aerial image data of the area (e.g., Fig 3). The aerial image data used are the original aerial images acquired by the RC30 aerial camera at a focal length of 153.022 mm. The flight altitude is 1650 m higher than the average ground elevation of the imaged area. The aerial photographs are initially recorded on film and then scanned into digital format at a pixel resolution of 25 μm. The DSM data are accurate to approximately 0.1 m and 0.2 m for planar and vertical coordinates, respectively, with a horizontal datum of GRS 1980 and a vertical datum of NAD83.

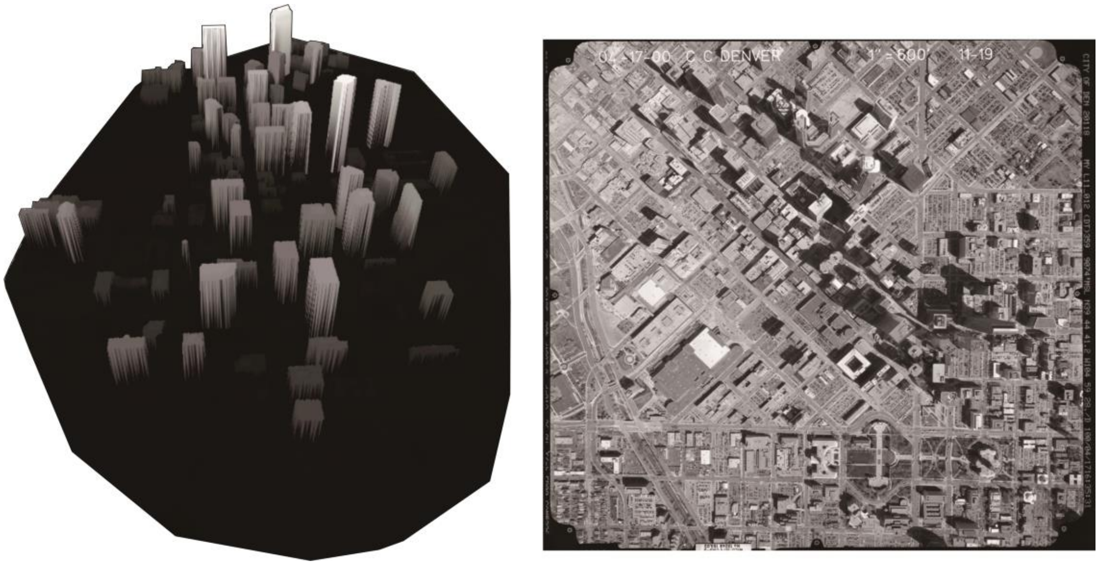

(a) DSM data

(b) Aerial images

Fig.3 Experimental data

3.2 Orthorectification results

Orthorectification is performed using aerial imagery and DSM raster data, and the EOPs are obtained by solving the whole set of ground control points uniformly arranged in the test area, and the pixel chunking method of this paper is used in the orthorectification process. The orthorectified result can be obtained as shown in Figure 4 below (the pixel chunk size used in the figure is 7*7 pixels).

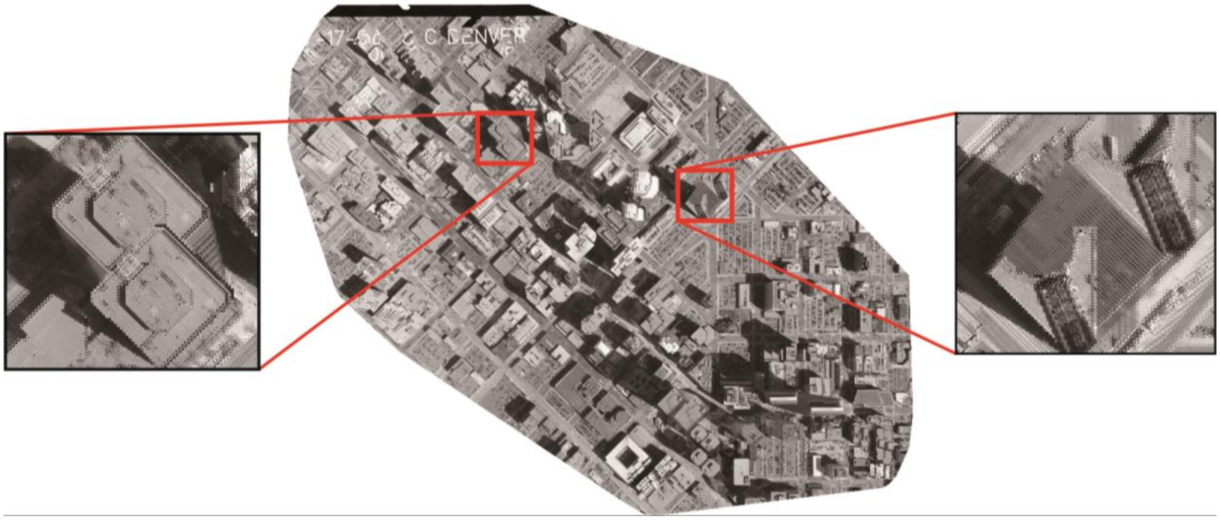

Fig.4 Orthorectification results for multi-pixel chunks (7*7 pixels chunk size as an example)

In order to observe the advantages and disadvantages of multi-pixel chunk correction under different chunk sizes for ortho correction results, experiments with a resolution of 1 m and six chunk sizes were conducted in this paper, as shown in Figures 5. One of the plots in the corrected result map was selected and magnified 500 times to observe its texture details. It can be clearly seen that there is almost no difference in texture detail and sharpness of the correction results at 3*3 and 5*5 pixels chunk sizes compared to the conventional pixel-by-pixel differential correction. The 7*7 pixels chunk size results in a certain checkerboard effect visible at 500x magnification, but the texture detail is not significantly missing and the edges of the features are clearly visible. The orthophoto results for the 9*9 pixels chunk size and larger chunks than that start to show a more pronounced lack of texture detail and the edges of the features become blurred due to the checkerboard effect, but the overall effect is more comparable to the pixel-by-pixel ortho correction with a resolution of 1 m.

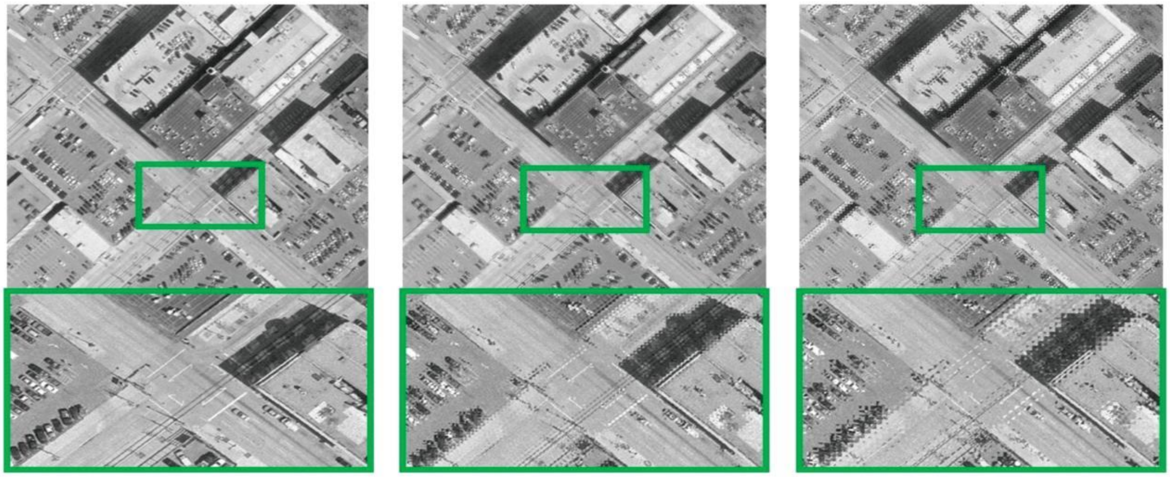

(a) Pixel-by-pixel correction (b) 3*3 pixels correction (c) 5*5 pixels correction

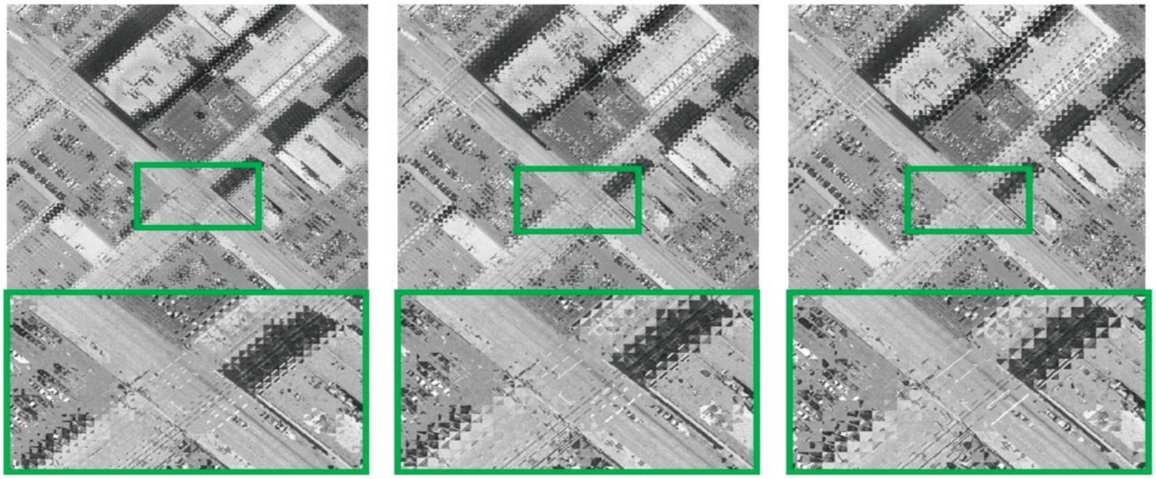

(d) 7*7 pixels correction (e) 9*9 pixels correction (f) 11*11 pixels correction

Fig.5 Ortho-corrected local effects in multi-pixel chunks (resolution of 1 m)

To facilitate the comparison of the efficiency and accuracy of multi-pixel chunking correction and pixel-by-pixel correction, the experiment shown in Figure 6 is conducted in this paper. In which pixel-by-pixel differential correction was applied to the experimental data at 1 m, 2 m, and 4 m resolution, and the time required for correction was 121.6 s, 73.68 s, and 29.93 s, respectively. In order to demonstrate the efficiency of multi-pixel chunk correction, the orthorectification results with a resolution of 1 m for a 5*5 pixels chunk size that took 20.02 s were selected in this paper. As can be seen from the figure, the pixel sharpness of the 5*5 pixels binning correction result used in this paper is significantly better than that of the conventional differential correction result with a resolution of 4 m, which requires essentially the same time, and the texture detail is richer than that of the conventional differential correction result with a resolution of 2 m.

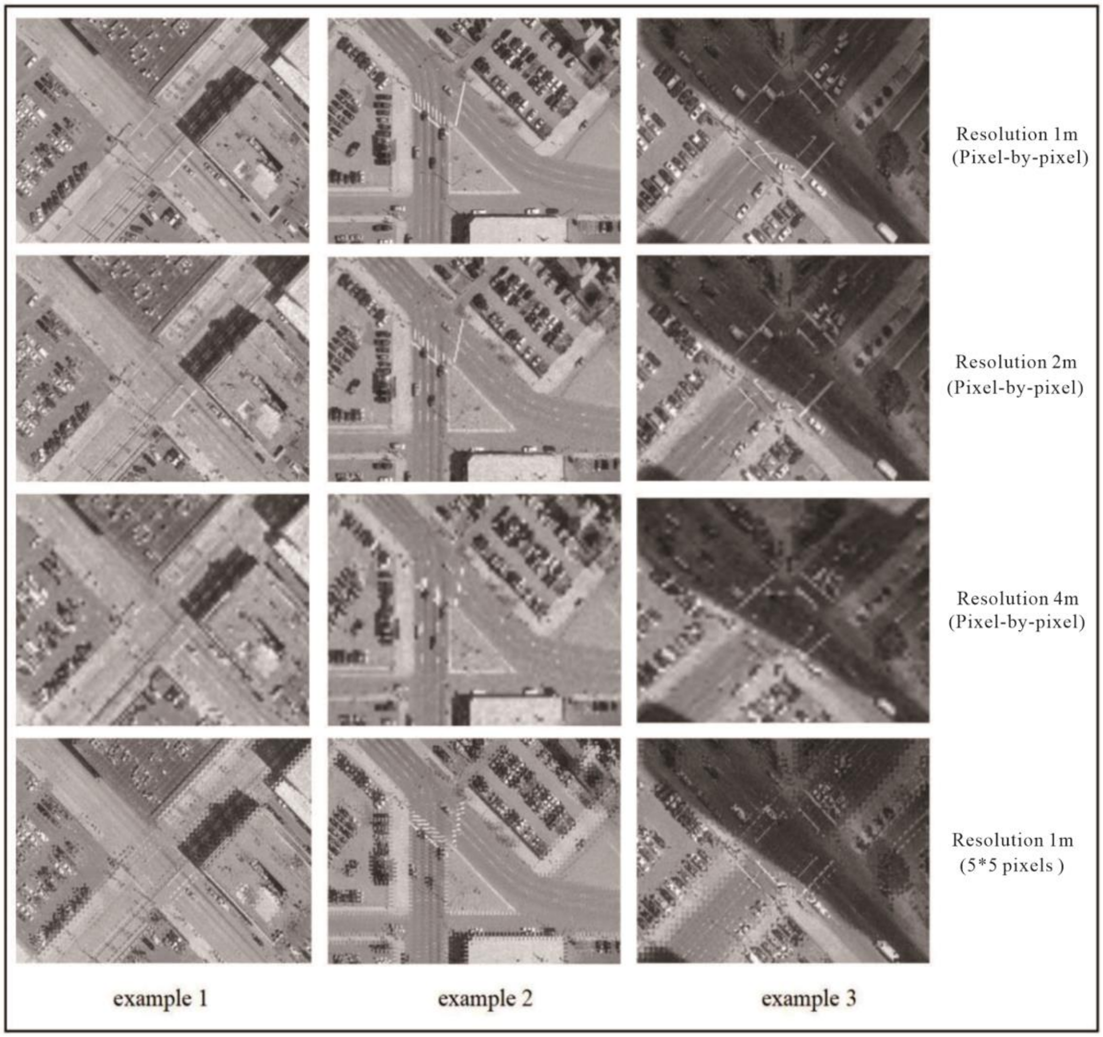

Fig.6 Comparison of pixel-by-pixel ortho-correction with different resolutions

3.3 Error analysis

Ten sample points were randomly collected on the orthophoto and the accuracy was calculated using the root mean square error formula. The calculated plane accuracy statistics of the plane accuracy of the ortho-correction method in this paper and the ortho-correction results of the conventional method are shown in Figure 7 and Table 1.

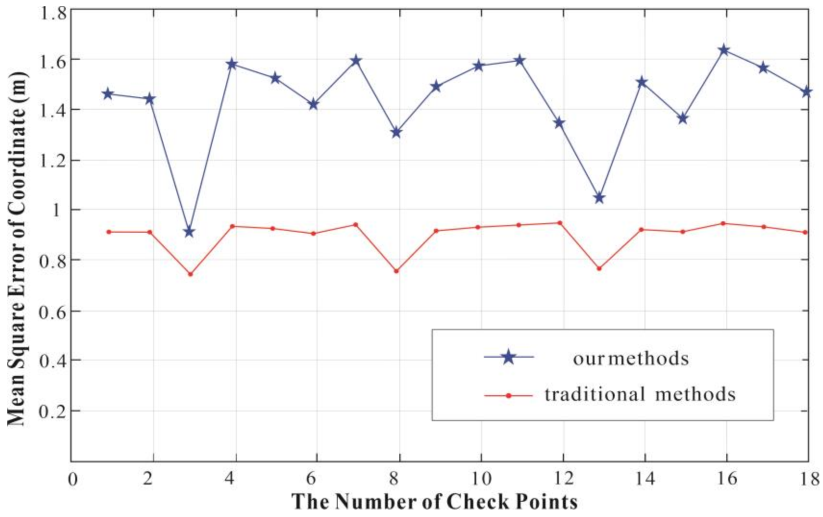

Fig.7 Line graph of plane error accuracy of this method and traditional method

Table1 Plane coordinate accuracy statistics table

	Max	Min	Mean	Standard Deviation
X coordinator	1.06 m	0.25 m	0.82 m	0.14 m
Y coordinator	1.82 m	0.73 m	1.53 m	0.38 m

From the above graph, we can see that the orthophoto plane accuracy of applying the adaptive chunking ortho correction method is about 0.4 m lower on average in the X-axis and 0.3 m lower on average in the Y-axis than that of the conventional ortho correction results. And the orthorectification results generated by this method are less than 1.6 m in-plane error, which meets the need of urban high-resolution image orthorectification production.

3.4 Processing Speed Comparison

First, the experimental data are orthorectified using the traditional pixel-by-pixel orthorectification method with an average time of 121.6s. While using the multi-pixel chunking orthorectification in this paper, the average elapsed time is 29.6s under the 3*3 chunking strategy. With a 7*7 chunking strategy, the average elapsed time is 13.4s. Time consumption includes only correction processing time. The method in this paper is 4.1 times faster than the traditional pixel-by-pixel method at 3*3 minimum chunking strategy and 9.5 times faster at 7*7 chunking strategy. It can be seen that the larger chunk, the faster the orthorectification speed using multi-pixel chunks for a certain number of pixels.

4. CONCLUSION

An orthorectification method based on multi-pixel chunking is proposed for real experimental verification of aerial images of Denver, and the following conclusions are obtained.

(1) The proposed multi-pixel chunking-based orthorectification method is feasible.

(2) It is proposed to perform orthorectification according to different chunk sizes to find the optimal correction accuracy and correction efficiency chunk size.

(3) The corrected image was checked using checkpoints and visual inspection, and the correction accuracy was 1.6 m. The correction accuracy met the ortho correction production requirements. Therefore, the results of this paper are reasonable for fast and efficient ortho-correction using multi-pixel chunking ortho-correction method.

(4) Since the correction of the method proposed in this paper for each chunk only considers two image points, the center and the bottom corner, and does not consider the elevation effects of other points. Therefore, when the chunks are large, the generated orthophoto is prone to misalignment and checkerboard effect in areas with large topographic relief.

Since the influence of topographic undulations in each sub-block is not considered, it will inevitably result in the loss of accuracy in the internal regions of the sub-blocks and the misalignment of the joint edges. Subsequent research will investigate the orthorectification method for high-precision multi-pixel chunking.

REFERENCES

[1] Herold M, Goldstein N C, Clarke K C. The spatiotemporal form of urban growth: measurement, analysis and modeling[J]. *Remote Sensing of Environment*, 2003, 86(3):286-302.

[2] Federal Geographic Data Committee. Fact Sheet: National Digital Geospatial Data Framework: A Status Report; Federal Geographic Data Committee: Reston, V A, USA, July 1997; 37p.

[3] Maitra, J.B. The National Spatial Data Infrastructure in the United States: Standards; Metadata, Clearinghouse, and Data Access; Federal Geographic Data Committee c/o US Geological Survey: Reston, V A, USA, 1998.

[4] Zhou, G.Q; Chen, W.; Kelmelis, J.; Zhang, D. Y.A comprehensive study on urban true orthorectification. *IEEE Trans. Geosci. Remote Sens*. 2005, 43, 2138–2147.

[5] Aguilar, M.A.; Saldaña, M.D.M.; Aguilar, F.J. Assessing geometric accuracy of the orthorectification process from GeoEye-1 and WorldView-2 panchromatic images. *Int. J. Appl. Earth Obs*. 2013, 21, 427–435.

[6] Habib, A.; Xiong, W.; Yang, F.; HeH, L.; Crawford, M. Improving orthorectification of UVA-based pushbroom scanner imagery using derived orthophotos from frame cameras. *IEEE J.-STARS* 2017, 10, 262-276.

[7] Ontiveros-Robles, E.; Vázquez, J.G.; Castro, J.R.; Castillo, O. A FPGA-based hardware architecture approach for real-time fuzzy edge detection. In *Nature-Inspired Design of Hybrid Intelligent Systems*; Melin, P., Castillo, O., Kacprzyk, J., Eds.; Springer International Publishing: Basel, Switzerland, 2017; pp. 519–540, ISBN 978-3-319-47054-2.

[8] Zhang, C.; Liang, T.; Mok, P.K.T.; Yu, W. FPGA implementation of the coupled filtering method. In Proceedings of the 2016 IEEE International Conference on Bioinformatics and Biomedicine (BIBM), Shenzhen, China, 15–18 December 2016; pp. 435–442.

[9] Shoab, M.; Singh, V.K.; Ravibabu, M.V. High-Precise True Digital Orthoimage Generation and Accuracy Assessment based on UA V Images. *J. Indian Soc. Remote Sens*. 2021, 50, 613–622.

[10] Zhou, G. Near Real-Time Orthorectification and Mosaic of Small UAV Video Flow for Time-Critical Event Response. *IEEE Trans. Geosci. Remote Sens*. 2009, 47, 739–747.

[11] Zhou G, Wang Q, Huang Y, et al. True2 Orthoimage Map Generation[J]. *Remote Sensing*, 2022, 14(17): 4396.

[12] Warpenburg, M.R.; Siegel, L.J. SIMD image resampling. *IEEE T rans. Comput*. 1982, 31, 934–942.

[13] Wittenbrink, C.M.; Somani, A.K. 2D and 3D optimal parallel image warping. In Proceedings of the Seventh International Parallel Processing Symposium, Newport, CA, USA, 13–16 April 1993; pp. 331–337.

[14] Liu, H.; Yang, J.; Liu, H.; Zhang, J. A new parallel ortho-rectification algorithm in a cluster environment. In Proceedings of the Third International Congress on Image and Signal Processing, Yantai, China, 16–18 October 2010; pp. 2080–2084.

[15] Dai, C.; Yang, J. Research on orthorectification of remote sensing images using GPU-CPU cooperative processing. In Proceedings of the International Symposium on Image and Data Fusion, Tengchong, China, 9–11 August 2011; pp. 1–4.

[16] Quan, J.; Wang, P.; Wang, H. Orthorectification of optical aerial images by GPU acceleration. *Opt. Precis. Eng*.2016, 24, 2863–2871.